

Application of Triple Collocation Technique to Wave Resource Assessments and Wave Energy Converter Energy Production

Bryson Robertson*, Yuhe Lin & Bradley Buckham
West Coast Wave Initiative, Institute of Integrated Energy Systems
University of Victoria, Canada
*bryson@uvic.ca

Abstract

Numerical wave propagation models are often used to hindcast wave conditions and predict the theoretical energy production from wave energy conversion (WEC) devices. It is widely acknowledged that numerical model suffer from bias's and uncertainties which ultimately affect the final predictions of WEC power. In this case study, a Simulating WAVes Nearshore (SWAN) model is used to predict sea states off the Canadian west coast and the triple collocation technique is applied to quantify the model result bias's, and systematic and random errors. To analyze the error and calibrate the SWAN model, two in-situ collocated wave measurement devices are deployed; A TRIAXYS wave measurement buoy and a Nortek AWAC. The triple collocation technique is used to compare the significant wave height and energy period parameters over a three month period, from October to December 2014. The triple collocation technique assumes linear relationship between the measured value and true value, and outputs the bias, calibration slope and the measurement random error. This study implements two previously utilized calibration regimes, a single value and monthly calibration regime, as well as presenting two novel methods to improve the impact of the calibration; a bivariate calibration and a spectral calibration. Given the short period of data collection, the two standard calibration techniques resulted in negligible improvements in data correlation. The bivariate calibration regime, following the IEC wave resource histogram parameters, resulted in 5% and 29% improvements in the significant wave height and energy period correlations respectively. The spectral method suffered from high computational cost and lower performance improvements that the bivariate regime. Applying the improved wave resource assessment data to WEC energy production increased the energy generation over the 3 month period by 15.9%, and reduced the under prediction SWAN bias to just 0.30% (when compared against the AWAC data). Annual energy production differed by 6% between calibrated SWAN data and original data – a significant amount when assessing large scale wave energy production.

1 Introduction

Numerical wave propagation models are often used to hindcast wave conditions over long time timelines and over large spatial areas. The multiyear results from these numerical models are often used as the sole input to detailed wave resource assessments for the wave energy industry. The spatial and temporal distribution of the hindcasted seastates are subsequently used to predict the theoretical energy production from wave energy conversion (WEC) devices. However, it is widely acknowledged that numerical models suffer from systematic biases and random uncertainties, which ultimately can significantly affect the predictions of WEC generated power and the feasibility of proposed wave energy development projects.

The numerical model biases and uncertainties result from a number of factors including, but not exclusive of, input boundary condition resolution, underlying physics assumptions, numerical errors, and insufficient bathymetric resolution. Additionally, many global wave models often assimilate current measurements from in-situ measurement devices [1], such as wave measurement buoys or acoustice wave and current profilers (AWAC), or remote measurements from satellite observations and radars. Thus, the inherent uncertainties within the numerical model can be compounded by uncertainties within the assimilated wave measurement data. Hence, it is import to be able to quantify both the errors and uncertainties associated with the model and the assimilated measurement data source, before utilizing the wave measurement to predict the power or annual energy productions from WEC's.

If three collocated measurements are available, the triple collocation technique has been widely used to estimate measurement errors and the systematic biases between three different data sources [2]–[7]. The technique is based on the assumption of a linear relationship between the measured value and true value, a normal distribution of error and the fact that the errors from each device are uncorrelated. Stoffelen [2] first used the triple collocation technique to estimate the error characteristics for each device and calibrate near surface wind speed from three collocated sources: wind buoys, an environmental forecast model, and European Remote-Sensing Satellite (ERS) scatterometer. Cairns and Sterl [3] built on this work and applied the triple collocation technique to validate both significant wave height and wind speed fields from European Centre for Medium Range Weather Forecasts (ECMWF) re-analysis ERA-40 against wave measurement buoys, ERS-1 scatterometer, and Topex altimeter. In their work, device uncertainties and calibration constants were determined on both an annual and latitude based matrix. More recently, Janssen's paper [4] compares wave height from ECMWF wave forecasting model to both buoy data and altimeter wave data from ERS-2. Janssen et al. suggest that monthly calibration parameters were necessary to capture the variation in the calibration coefficients.

In order to assess the impact of model and device uncertainties on annual WEC energy production, this study investigates the impact of model and device uncertainty under four differing calibration regimes. Initially, the impacts of model calibration under the regimes suggested by both Cairns and Sterl [5] and Janssen et al. [6] are quantified. Subsequently, two novel model calibration regimes are introduced and their performance quantified; one based on a bivariate distribution of significant wave heights and energy periods, while the other utilizes the entire frequency domain variance density spectrum.

The paper is structured as follows: Section 2 details the database of SWAN, buoy and AWAC measurements used as inputs to the triple collocation technique. In Section 3, a brief overview of methodology applied as part of the triple collocation technique is presented and discussed. Section 4 presents the calibration regimes investigated and the differences in the resulting bias, beta and uncertainty values are discussed. The correlation impact of the differing calibration regimes, and a discussion of regime limitations, is presented in Section 5. Section 6 explores the impact of the triple collocation method on wave energy period and presents results on the variation in energy production from wave energy converters. Section 7 and Section 8 discuss the inconsistencies in the study results and presents conclusion's respectively.

2 Wave Measurements and Models

The West Coast Wave Initiative at the University of Victoria runs an unstructured Simulating Waves Nearshore (SWAN) model for the west coast of Vancouver Island in order to provide a 10 year hindcast of wave conditions [8]. SWAN is a third generation phase-averaged Eulerian numerical wave model designed to simulate the propagation of waves in shallow near-shore areas [9]. Within the region of interest for this triple collocation study, the model spatial resolution is $\sim 100\text{m/node}$, has 3 hr temporal resolution, the variance density spectrum features 36 frequency bins, between 0.035Hz and 1.00 Hz, and 3° directional resolution [10]. The hindcast utilizes offshore wave conditions provided by the European Centre for Medium Range Weather Forecasts (ECMWF) and wind forcing inputs from the Fleet Numerical Meteorology and Oceanographic Centre (FNMOC) COAMPS model.

In order to apply the triple collocation technique [5][6], two wave measurement devices were deployed. These include an AXYS Technologies TRIAXYS wave measurement buoy and a Nortek Acoustic Wave And Current (AWAC) profiler. These devices were collocated at Port Renfrew, British Columbia, Canada during September - December 2014 in $\sim 30\text{m}$ of water. The TRIAXYS buoy utilizes rate gyros and accelerometers to record the buoy motions, due to surface interactions with incoming waves, and calculate the directional wave spectrum. Conversely, the AWAC is a seafloor mounted device and utilizes measurements of the fluid velocities close to the water surface in order to recreate the directional wave spectrum. The buoy data has a 20 minute temporal resolution with a 0.005 Hz spectral and 3° directional resolution, while the AWAC data is at a 1 hour temporal resolution and a 0.01 Hz spectral and 2° directional resolution.

Figure 1 presents the significant wave height from the buoy, AWAC, and SWAN between October 1st and December 31st, 2014.

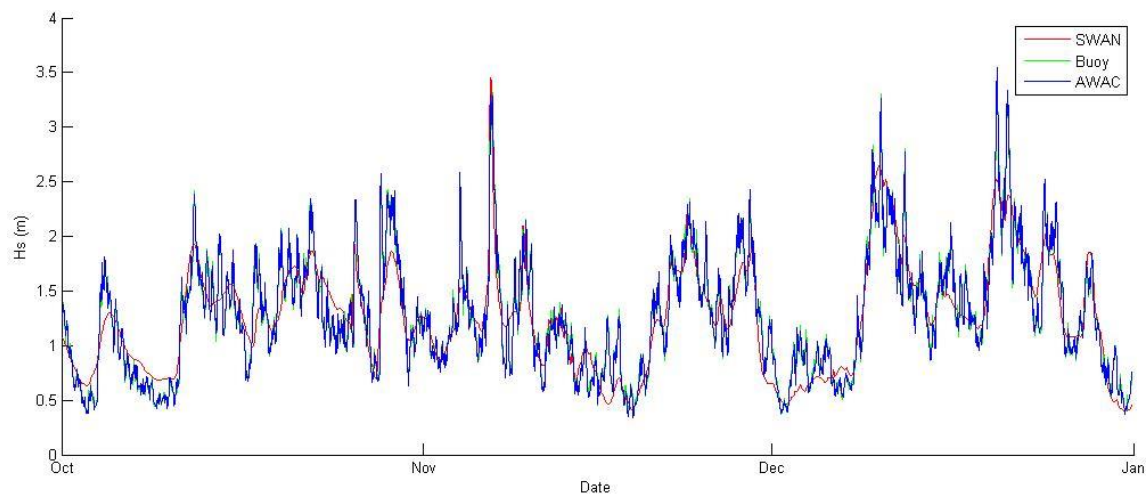


Figure 1: Raw significant wave heights from SWAN model, AWAC and TriAxys buoy

Figure 2 illustrates the high degree of correlation between the two measurement devices (buoy and AWAC), while Figure 3 indicates the significant scatter when comparing the SWAN model against the AWAC data. The AWAC and buoy data feature a correlation of 0.97, a root mean square error (RMSE) of just 0.12 and a scatter index (SI) of 0.10. As shown in Figure 2, the linear fit (with a zero intercept) follow the perfect agreement line very closely. Conversely, a comparison of the AWAC and SWAN model data shows significant scatter (SI = 0.20) and has a lower correlation of 0.89. In general, the SWAN model linear fit line indicates a general under prediction of wave heights, increasing with height.

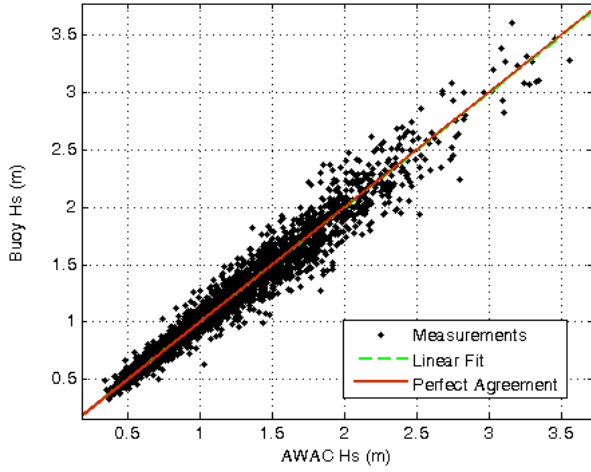


Figure 2: Scatter plot for AWAC H_s and buoy H_s

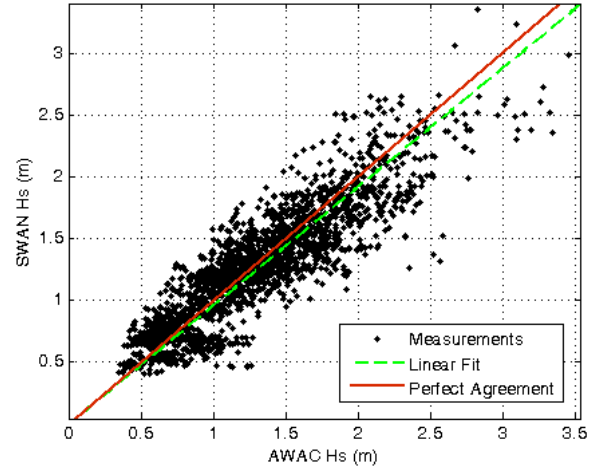


Figure 3: Scatter plot for AWAC H_s and SWAN H_s

To calibrate the SWAN model, and quantify the bias and errors associated with each measurement device, the triple collocation technique will be utilized. Given that the two devices are measuring two different physical processes associated with waves, it is assumed that they have uncorrelated errors.

3 Triple Collocation Methodology

Triple collocation technique has been widely used to estimate uncertainty of measurements from three different, yet collocated, data sources. Triple collocation technique is based on the assumption of a linear relationship between the measured value and true value, and can be expressed in the following equations:

$$\begin{aligned} X &= \alpha_x + \beta_x T + e_x \\ Y &= \alpha_y + \beta_y T + e_y \\ Z &= \alpha_z + \beta_z T + e_z \end{aligned} \quad (1)$$

where T is the true value, α and β are unknown calibration parameters representing bias and linear calibration coefficient (beta) respectively, e is uncertainty of the data. Given that the true value is unknown, this method requires that one of the datasets is defined as the reference and the other two data sets will be calibrated it. However, as noted by Janssen et al.[6], the choice of T is doesn't affect the results. Janssen et al. additionally removed the α values from (1), arguing that significant wave height is a positive definite quantity and incorrect calibration constants may result in negative predictions of significant wave height. For this study, α values were included, and the respective influence detailed in proceeding sections. The AWAC was defined as the reference dataset; hence the beta and bias will be set to 1 and 0 respectively.

The first step removes of the bias from the datasets by introducing the following new variables,

$$\begin{aligned} X' &= X - \alpha_x \\ Y' &= Y - \alpha_y \\ Z' &= Z - \alpha_z \end{aligned} \quad (2)$$

A new set of equations, without T, result from inserting (2) into (1). The uncertainty term e in (1) can be modified to:

$$\begin{aligned} X'' - T &= \frac{X'}{\beta_x} - T = \frac{e_x}{\beta_x} = e_x'' \\ Y'' - T &= \frac{Y'}{\beta_y} - T = \frac{e_y}{\beta_y} = e_y'' \\ Z'' - T &= \frac{Z'}{\beta_z} - T = \frac{e_z}{\beta_z} = e_z'' \end{aligned} \quad (3)$$

By calculating the difference between any two of above equations, the true value can be eliminated:

$$\begin{aligned} X'' - Y'' &= e_x'' - e_y'' \\ Z'' - Y'' &= e_z'' - e_y'' \\ X'' - Z'' &= e_x'' - e_z'' \end{aligned} \quad (4)$$

Error terms can then be calculated by multiplying any of the two equations above, with the assumption that all the covariances are equal to 0. This assumption is valid if the errors in the three collocated measurements are independent to each other. As shown in (5), the uncertainty term is independent from the choice of reference (where $\bar{\quad}$ denotes mean value):

$$\begin{aligned} (\overline{X''} - \overline{Y''}) \cdot (\overline{Z''} - \overline{Y''}) &= (e_x'' - e_y'') \cdot (e_z'' - e_y'') = (e_y'')^2 \\ (\overline{X''} - \overline{Z''}) \cdot (\overline{Y''} - \overline{Z''}) &= (e_x'' - e_z'') \cdot (e_y'' - e_z'') = (e_z'')^2 \\ (\overline{X''} - \overline{Z''}) \cdot (\overline{X''} - \overline{Y''}) &= (e_x'' - e_z'') \cdot (e_x'' - e_y'') = (e_x'')^2 \end{aligned} \quad (5)$$

Used the same methodology from Janssen et al [4], following the works of Marsden [11], a neutral regression can be used to calculated beta according to (6):

$$\beta_y = (-B + \frac{\sqrt{B^2 - 4AC}}{2A}) \quad (6)$$

where $A = \gamma \overline{X'Y'}$, $\gamma = \frac{\overline{e_x}}{\overline{e_y}}$, $B = \overline{X'^2} - \gamma \overline{Y'^2}$, $C = -\overline{X'Y'}$. Of course, β_z can be obtained by changing all the y terms to z in (6). The bias can then calculated from beta using:

$$\begin{aligned} \alpha_y &= \overline{Y} - \beta_y \overline{X} \\ \alpha_z &= \overline{Z} - \beta_z \overline{X} \end{aligned} \quad (7)$$

However, the above equations start with unknown parameters α_y and α_z and end with calculating the same parameters, therefore iterative method can be implemented using the following assumed initial values:

$$\begin{aligned} \alpha_y &= \alpha_z = 0 \\ \beta_y &= \beta_z = 1 \end{aligned} \quad (8)$$

The iterative processes ends when either of the bias, beta, or error variance convergence. For this study, convergence was based on the error variance.

At this stage, it should be noted that Janssen et al. [6] removed the bias terms in (1), given that significant wave height is a positive definite quantity. Over the following sections, the impact of negative bias and monthly static calibration constants will be discussed.

4 Triple Collocation Application Regimes

As previously noted, the generic triple collocation technique has been applied to numerous oceanographic applications. For this study, a variety of differing calibration regimes were tested to determine which provided the best performance against the dataset. These regimes included:

- 1) Single value calibration.
- 2) Monthly calibration.
- 3) Bivariate calibration.
- 4) Spectral calibration.

The buoy, AWAC and SWAN data from the period October 1st, 2014, 00:00 to December 31st, 2015, 04:00 were used. It is acknowledged that a more extensive database would be valuable; unfortunately additional data is unavailable for this site.

The correlation between the uncalibrated and calibrated significant wave height is used as the metric to evaluate the calibration performance, under the four differing regimes. Expansion to include energy period will occur in Section 5, once the best performing calibration regime is determined. As previously noted, AWAC data has been widely used to validate buoy measurements [5], [12] and it will be used as the primary reference data source for all regimes.

4.1 Single calibration

Caires and Sterl [5] suggest calibrating data on both annual and latitude basis. Given the stationarity and short data time period investigated in this study, this would result in a single value to calibrate the three datasets. Following this application regime, Table 1 presents the calibration parameters in terms of bias, beta and error variance for each dataset, with respect to the corresponding reference dataset.

Table 1: H_s calibration results under the single value calibration regime

| Reference Data | Test | Bias (m) | Beta | Variance (m ²) | Normalized SD (%) |
|----------------|-------------|----------|----------|----------------------------|-------------------|
| AWAC | AWAC | 0 | 1 | 3.46e-04 | 1.45 |
| | SWAN | 0.032 | 0.99 | 5.41e-02 | 18.0 |
| | Buoy | 0.002 | 1.00 | 2.60e-04 | 1.26 |
| SWAN | AWAC | -0.032 | 1.01 | 3.42e-04 | 1.45 |
| | SWAN | 0 | 1 | 5.37e-02 | 17.9 |
| | Buoy | -0.031 | 1.01 | 2.60e-04 | 1.26 |
| Buoy | AWAC | -0.150 | 0.99 | 3.47e-04 | 1.46 |
| | SWAN | 0.030 | 0.99 | 5.42e-02 | 18.0 |
| | Buoy | 0 | 1 | 2.60e-04 | 1.26 |

The AWAC and buoy have bias and beta values close to 0 and 1 respectively, when compared against the bias and beta associated with the SWAN data. Moreover, the normalized standard deviation (SD) of error for AWAC and buoy are within 1.5%, while SWAN has values around 18%. This confirms the visual observations from Figure 1; that the AWAC and buoy is more accurate than data from SWAN. Additionally, it can be noted from Table 1, that the measurement error variance is independent from the choice of reference dataset.

As noted by Janssen et al, in the single value calibration regime, there are several occasions when the measurement bias is significantly negative; this could lead to negative significant wave heights once the measurements have been calibrated. In this calibration regime, the validity of the triple collocation technique, with a bias factor, is questionable and the methods followed by Janssen et al. may be better suited.

4.2 Monthly calibration

Following the methodology presented by Janssen et al.[6], the second test regime investigates monthly significant wave height calibrations of the three datasets. The three months of data were divided and independently used in the triple collocation procedure. Table 2 presents the monthly bias, beta and error variance results, while Figure 4 and Figure 5 provide a visual representation of the data. The bias and beta values vary for each month by month while the variance remains fairly constant. The device measurement error variance estimates are similar to those determined in the single calibration regime.

Table 2: H_s calibration results under the monthly calibration regime

| Month | Test | Bias (m) | Beta | Variance (m ²) |
|----------|-------------|-----------|----------|----------------------------|
| October | AWAC | 0 | 1 | 1.60e-04 |
| | SWAN | 4.01e-02 | 0.982 | 5.91e-02 |
| | Buoy | 8.81e-04 | 1.00 | 3.13e-04 |
| November | AWAC | 0 | 1 | 5.02e-04 |
| | SWAN | -1.63e-03 | 0.983 | 4.66e-02 |
| | Buoy | 6.62e-03 | 1.00 | 1.94e-04 |
| December | AWAC | 0 | 1 | 4.52e-04 |
| | SWAN | 2.20e-02 | 1.00 | 5.50e-02 |
| | Buoy | 1.90e-03 | 1.00 | 1.96e-04 |

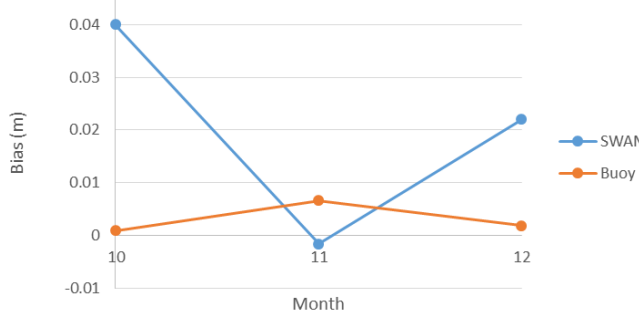


Figure 4: Monthly bias values for SWAN and buoy data

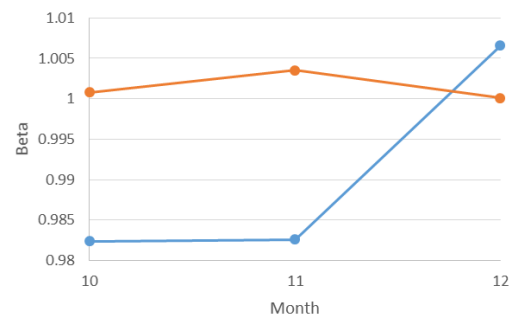


Figure 5: Monthly beta values for SWAN and buoy data

As in the single value calibration regime, the presence of negative bias values is noted in Table 2. However, the bias values are significantly minimized from those presented in the single value calibration regime, thus reducing the risk of calibration resulting in negative significant wave height values.

4.3 Bivariate calibration

For this section, the triple collocation technique will be applied on two different SWAN model datasets, one at the baseline model completed at 3hr resolution [13] and another a specific model run at 1 hr temporal resolution.

4.3.1 Application to baseline SWAN dataset

In an effort to improve the performance of the triple collocation technique and the correlation between the datasets, the third test regime applied the triple collocation technique to the individual wave height and period bins utilized in a standard wave resource assessment histogram. The International Electrotechnical Commission (IEC) has released a series of standards and technical specifications to help the wave energy conversion (WEC) industry develop and provide consistency across the main device architectures and global development efforts. The IEC Wave Resource Assessment and Characterisation Technical Specification [14] calls for a bivariate histogram of annual wave conditions, based on 0.5m significant wave height and 1s energy period bins.

Table 3: Number of observation hours for baseline SWAN model (Red: non-convergent cell or cell with less than 50 occurrences; Green: convergence cell; Yellow: no data in the cell)

| | | Energy Period - T_e (s) | | | | | | | |
|-----------|---------|---------------------------|---|----|-----|-----|----|----|----|
| | | 1 | 3 | 5 | 7 | 9 | 11 | 13 | 15 |
| H_s (m) | 0-1.0 | 0 | 1 | 65 | 100 | 78 | 4 | 0 | 0 |
| | 1.0-2.0 | 0 | 0 | 23 | 59 | 218 | 98 | 14 | 2 |
| | 2.0-3.0 | 0 | 0 | 0 | 6 | 29 | 25 | 7 | 1 |
| | 3.0-4.0 | 0 | 0 | 0 | 0 | 2 | 2 | 0 | 0 |
| | 4.0-5.0 | 0 | 0 | 0 | 0 | 0 | 0 | 0 | 0 |

For the initial efforts within this test regime, the baseline 3 hr SWAN model results were used. The significant wave height data was binned according to the IEC technical specification [14], and the triple collocation technique applied to individual bins in the histogram. As a result, significant wave height and energy period specific bias, beta and error variance values were determined. However, due to a low number of occurrences for specific wave height and period bins, the triple collocation technique was unable to converge and no reliable results were found. By doubling both the significant wave height and energy period bins widths, in order to increase the number of data points in each bin, allowed for convergence to occur in multiple histogram bins. Table 3 presents the convergence results for the reduced histogram.

To reduce the error variance caused by the lack of data and convergence, all bins which did not converge or featured less than 50 occurrences was deemed of questionable value and were removed from the analysis. Unfortunately, this filtering only left 3 bins with sufficient number of data points and quality. The bias and beta in the convergence bin are shown in the Table 4, Table 5, Table 6, and Table 7. It is noticed both the SWAN and buoy datasets generally have beta values closer to 1 and bias value closer to 0 as the significant wave height increases from 0.5m to 1.5m. This indicates greater correlation with the measurements from the AWAC at larger wave heights. As expected, the buoy data continues to present bias and beta values closer to 1 and 0 respectively, when compared against the SWAN data.

| SWAN | | Beta | | | | | | | |
|-----------|------|-----------|---|---|--------|--------|----|----|----|
| | | T_e (s) | | | | | | | |
| | | 1 | 3 | 5 | 7 | 9 | 11 | 13 | 15 |
| H_s (s) | 0.50 | | | | 1.1415 | 1.2772 | | | |
| | 1.50 | | | | | 0.9917 | | | |
| | 2.50 | | | | | | | | |
| | 3.50 | | | | | | | | |

Table 4: SWAN model beta obtained under bivariate calibration regime (3 hour time step SWAN)

| Buoy Beta | | Beta | | | | | | | |
|-----------|------|-----------|---|---|--------|--------|----|----|----|
| | | T_e (s) | | | | | | | |
| | | 1 | 3 | 5 | 7 | 9 | 11 | 13 | 15 |
| H_s (s) | 0.50 | | | | 1.0006 | 1.0073 | | | |
| | 1.50 | | | | | 0.9968 | | | |
| | 2.50 | | | | | | | | |
| | 3.50 | | | | | | | | |

Table 5 : Buoy beta obtained under bivariate calibration regime (3 hour time step SWAN)

| SWAN | | Bias | | | | | | | |
|-----------|------|-----------|---|---|--------|--------|----|----|----|
| | | T_e (s) | | | | | | | |
| | | 1 | 3 | 5 | 7 | 9 | 11 | 13 | 15 |
| H_s (s) | 0.50 | | | | 0.0088 | 0.0129 | | | |
| | 1.50 | | | | | 0.0198 | | | |
| | 2.50 | | | | | | | | |
| | 3.50 | | | | | | | | |

Table 6: SWAN model bias obtained under bivariate calibration regime (3 hour time step SWAN)

| Buoy Bias | | Bias | | | | | | | |
|-----------|------|-----------|---|---|--------|---------|----|----|----|
| | | T_e (s) | | | | | | | |
| | | 1 | 3 | 5 | 7 | 9 | 11 | 13 | 15 |
| H_s (s) | 0.50 | | | | 0.0000 | -0.0006 | | | |
| | 1.50 | | | | | 0.0003 | | | |
| | 2.50 | | | | | | | | |
| | 3.50 | | | | | | | | |

Table 7: Buoy bias obtained under bivariate calibration regime (3 hour time step SWAN)

4.3.2 Application to hourly SWAN dataset

Given the low number of converged bins in the previous section, and in an effort to improve the impact of the triple collocation method, a study specific SWAN model run with 1 hour time resolution was completed. As a result, the number of available SWAN data points was tripled and the standard histogram, with 0.5 m H_s and 1s T_e resolution, could be used. The hourly convergence matrix is shown in Table 8 below.

Table 8: Number of observation hours for hourly SWAN model (Red: non-convergent cell or cell with less than 50 occurrences; Green: convergence cell; Yellow: no data in the cell)

| | | Energy Period - Te (s) | | | | | | | | | | | | | | | |
|--------|-------|------------------------|---|---|---|----|----|----|-----|-----|-----|-----|----|----|----|----|----|
| | | 1 | 2 | 3 | 4 | 5 | 6 | 7 | 8 | 9 | 10 | 11 | 12 | 13 | 14 | 15 | 16 |
| Hs (m) | 0-0.5 | 0 | 0 | 0 | 0 | 8 | 8 | 8 | 20 | 30 | 10 | 0 | 0 | 0 | 0 | 0 | 0 |
| | 0.5-1 | 0 | 0 | 0 | 1 | 86 | 91 | 85 | 192 | 142 | 48 | 10 | 2 | 0 | 0 | 0 | 0 |
| | 1-1.5 | 0 | 0 | 0 | 0 | 39 | 39 | 45 | 79 | 225 | 209 | 80 | 40 | 4 | 2 | 0 | 0 |
| | 1.5-2 | 0 | 0 | 0 | 0 | 0 | 1 | 8 | 33 | 111 | 119 | 101 | 62 | 29 | 10 | 4 | 0 |
| | 2-2.5 | 0 | 0 | 0 | 0 | 0 | 0 | 3 | 14 | 28 | 51 | 40 | 27 | 9 | 5 | 1 | 0 |
| | 2.5-3 | 0 | 0 | 0 | 0 | 0 | 0 | 0 | 3 | 5 | 8 | 4 | 0 | 6 | 2 | 1 | 0 |
| | 3-3.5 | 0 | 0 | 0 | 0 | 0 | 0 | 0 | 1 | 1 | 4 | 2 | 2 | 2 | 3 | 0 | 0 |
| | 3.5-4 | 0 | 0 | 0 | 0 | 0 | 0 | 0 | 0 | 0 | 0 | 0 | 0 | 0 | 1 | 0 | 0 |

With the increased temporal resolution SWAN dataset, the number of cells with both greater than 50 occurrences and achieve convergence increased to 11 from the 3 in the previous test regime. The resulting calibration parameters for convergence bins are shown in the tables below.

Table 9: SWAN model beta obtained under bivariate calibration regime (1 hour time step SWAN)

| SWAN Beta | | Energy Period (s) | | | | | | | |
|-----------|-------|-------------------|--------|--------|--------|--------|--------|--------|----|
| | | 6 | 7 | 8 | 9 | 10 | 11 | 12 | 13 |
| Hs (m) | 0-0.5 | | | | | | | | |
| | 0.5-1 | | 1.0276 | 1.1276 | 1.2284 | | | | |
| | 1-1.5 | | | 0.9506 | 1.0107 | 1.0477 | | | |
| | 1.5-2 | | | | 0.9061 | 0.9079 | 0.9731 | 1.0022 | |
| | 2-2.5 | | | | | 0.8751 | | | |
| | 2.5-3 | | | | | | | | |

Table 10: SWAN model bias obtained under bivariate calibration regime (1 hour time step SWAN)

| SWAN Bias | | Energy Period (s) | | | | | | | |
|-----------|-------|-------------------|--------|--------|--------|--------|--------|--------|----|
| | | 6 | 7 | 8 | 9 | 10 | 11 | 12 | 13 |
| Hs (m) | 0-0.5 | | | | | | | | |
| | 0.5-1 | | 0.0083 | 0.0089 | 0.0121 | | | | |
| | 1-1.5 | | | 0.0060 | 0.0058 | 0.0079 | | | |
| | 1.5-2 | | | | 0.0015 | 0.0023 | 0.0039 | 0.0021 | |
| | 2-2.5 | | | | | 0.0011 | | | |
| | 2.5-3 | | | | | | | | |

Table 11: Buoy beta obtained under bivariate calibration regime (1 hour time step SWAN)

| Buoy Beta | | Energy Period (s) | | | | | | | |
|-----------|-------|-------------------|--------|--------|--------|--------|--------|--------|----|
| | | 6 | 7 | 8 | 9 | 10 | 11 | 12 | 13 |
| Hs (m) | 0-0.5 | | | | | | | | |
| | 0.5-1 | | 1.0094 | 1.0058 | 1.0076 | | | | |
| | 1-1.5 | | | 1.0015 | 1.0016 | 0.9989 | | | |
| | 1.5-2 | | | | 1.0000 | 0.9962 | 0.9960 | 1.0006 | |
| | 2-2.5 | | | | | 0.9925 | | | |
| | 2.5-3 | | | | | | | | |

Table 12: Buoy bias obtained under bivariate calibration regime (1 hour time step SWAN)

| Buoy Bias | | Energy Period (s) | | | | | | | |
|-----------|-------|-------------------|--------|---------|---------|---------|---------|--------|----|
| | | 6 | 7 | 8 | 9 | 10 | 11 | 12 | 13 |
| Hs (m) | 0-0.5 | | | | | | | | |
| | 0.5-1 | | 0.0007 | 0.0004 | -0.0009 | | | | |
| | 1-1.5 | | | -0.0004 | -0.0002 | 0.0001 | | | |
| | 1.5-2 | | | | -0.0004 | 0.0010 | -0.0006 | 0.0000 | |
| | 2-2.5 | | | | | -0.0004 | | | |
| | 2.5-3 | | | | | | | | |

In terms of general observations, it appears that both the SWAN and buoy datasets feature beta values larger than 1 in low h_s regions and lower than 1 values in the larger h_s region. Moreover, the bias' for the SWAN dataset tend to decrease as h_s increases, indicating that SWAN over predicts h_s in low h_s situations and under predicts in larger h_s situations. This confirms the visual observations made in Figure 1. While the buoy calibration does result in negative bias values, the magnitudes are extremely small and would generally be unable to cause calibrated negative significant height values. Thus, when applied in the correct calibration regime, the inclusion of the bias terms in (1) seems justified.

Table 19 presents the normalized error SD's for each bin. If a single value regime was used, as per Caires and Sterl [5], the overall normalized error SD is 17.9% - slightly larger than the mean normalized error SD of 15% below.

| Hs % Uncertainty | | Energy Period (s) | | | | | | | | | |
|---------------------|-------|-------------------|---|-------|-------|-------|-------|-------|-------|----|--|
| | | 5 | 6 | 7 | 8 | 9 | 10 | 11 | 12 | 13 | |
| Hs (m) | 0-0.5 | | | | | | | | | | |
| | 0.5-1 | | | 19.48 | 15.28 | 14.72 | | | | | |
| | 1-1.5 | | | | 16.38 | 11.84 | 13.82 | | | | |
| | 1.5-2 | | | | | 15.01 | 18.76 | 13.04 | 10.17 | | |
| | 2-2.5 | | | | | | 16.75 | | | | |
| | 2.5-3 | | | | | | | | | | |

Table 13: Hs normalized error SD using bivariate regime

4.4 Spectral calibration

In an effort to further increase the performance of the triple collocation technique, the final regime attempts to determine the calibration parameters for each variance density bin within the frequency domain spectrum. The non-directional spectrums are binned into variance density or energy bins and the triple collocation technique was applied within each bin. This method significantly increased the size of the analysed data set size and allowed for better convergence. Figure 6 illustrates that convergence was achieved within the majority of the energy and frequency bins.

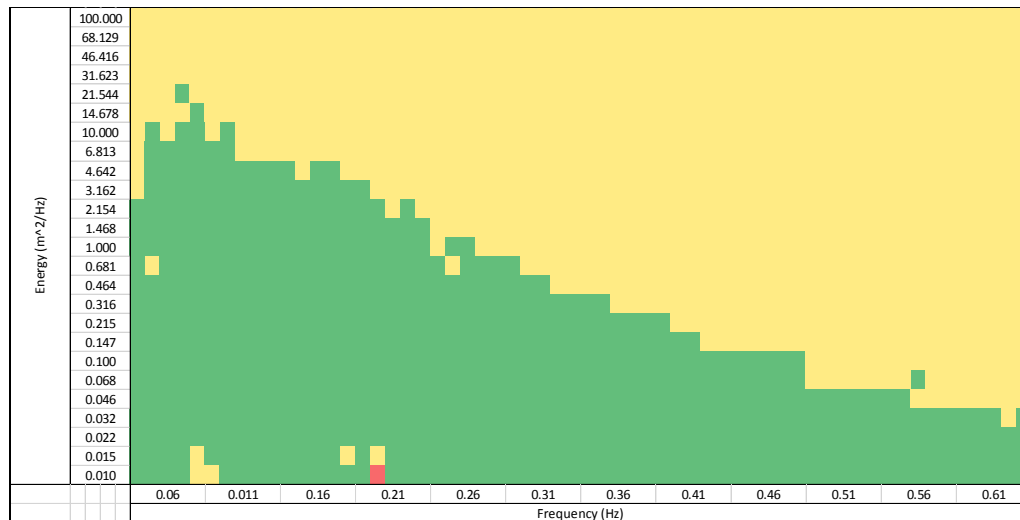


Figure 6: Spectral calibration regime convergence (1 hour time step SWAN)

The calibration parameters are shown in the figures below. It can be observed that the beta values for SWAN are bigger than 1 for most of the bins (reaching a maximum at 20), the bias values become increasingly negative in the lower frequency bands and the normalized error SD rises rapidly in the high

frequency/high energy bins. As may be expected, the buoy maintains beta values close to 1 (with the exception of low frequency/low energy bins), maintain a bias of ~ 0 and only featured significant variance in low frequency bins.

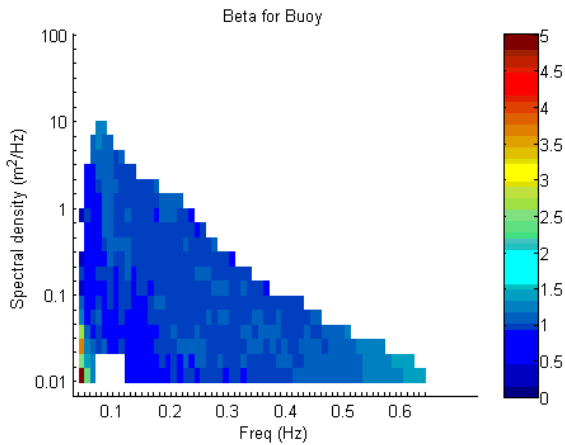


Figure 7: Buoy beta obtained under spectral calibration regime

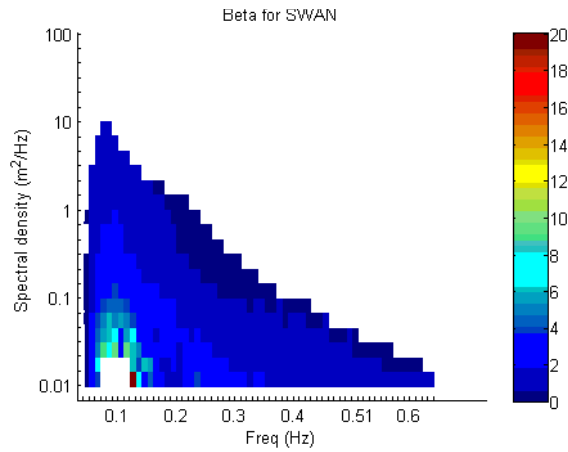


Figure 8: SWAN beta obtained under spectral calibration regime

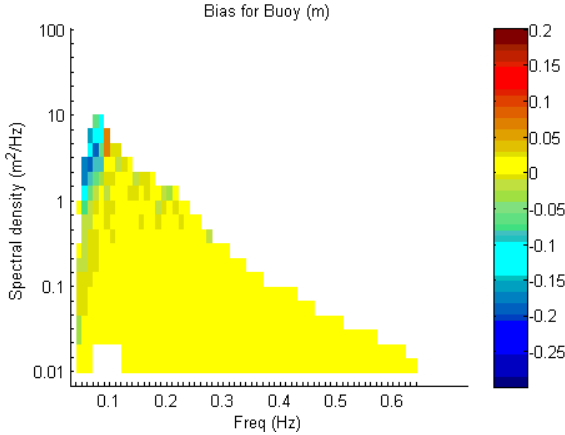


Figure 9: Buoy bias obtained under spectral calibration regime

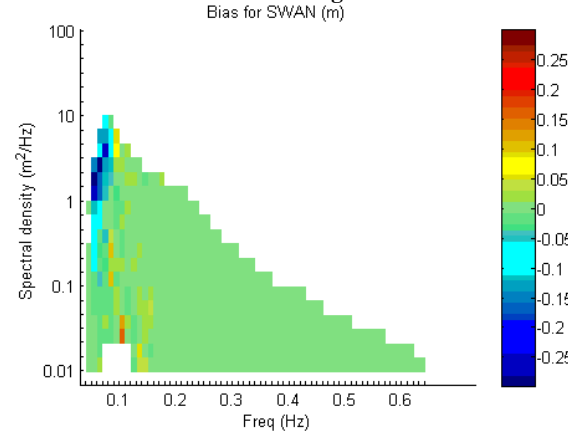


Figure 10: SWAN bias obtained under spectral calibration regime

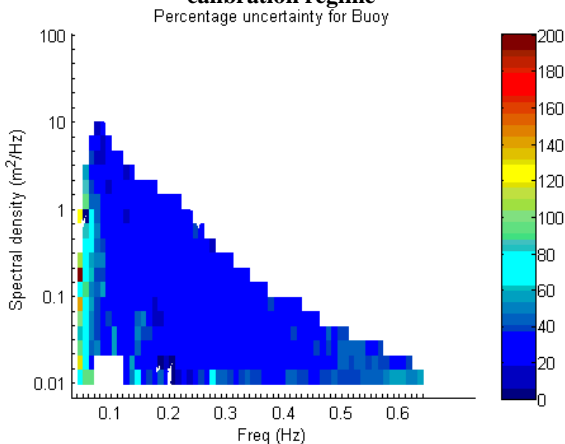


Figure 11: Buoy normalized error SD obtained under spectral calibration regime

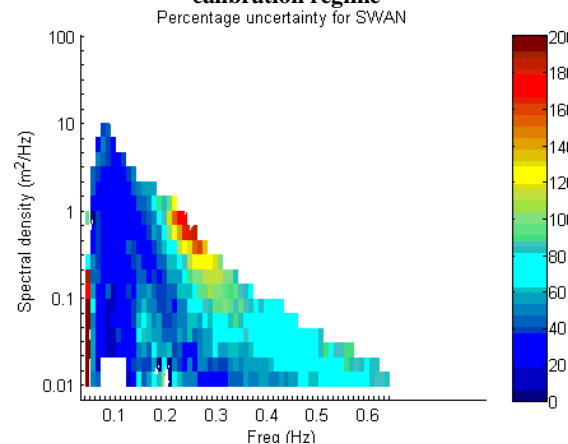


Figure 12: SWAN normalized error SD obtained under spectral calibration regime

In Figure 12, the normalized error SD for SWAN model is larger than 30% in majority of the bins, and reaches more than 100 percent in specific locations, which is significantly higher than the 18% for H_s obtained from single value test regime (See Table 1).

5 Test Regime Performance

5.1 Single calibration

Figure 13 shows the AWAC measurements, the raw uncalibrated SWAN model outputs and the calibrated SWAN model results. The raw and calibrated SWAN model results are almost identical and no improvement is realized. As a result, it is determined that the triple collocation technique provides little to no improvements in the performance of the SWAN model under the single value calibration regime. The correlation between the two datasets remained constant at 0.897 and the RMSE constant at 0.234. The only significant change resulting from the calibration was a reduction in the mean bias from 2cm to 3mm.

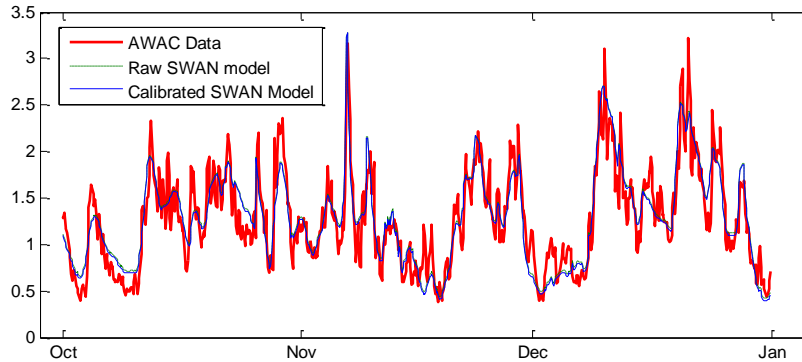


Figure 13: H_s values under the single value calibration regime

The triple collocation technique relies on the assumption of a normal distribution of error. As a double check, the SWAN model error SD resulting from the triple collocation technique is plotted in Figure 14 below. The yellow region represents a single SD on the SWAN model data, while the blue region indicates a double application of SD on the SWAN model data. Based on the assumption of a normal distribution of error, 95% of the AWAC data points should be included within the blue band. 94.3% of measured AWAC data points fall within the ideal 95th percentile confidence interval. Correspondingly, 71.4% of measured data points fall within the 67th percentile. This quick double check provides confidence that the error is normally distributed and the assumption is valid.

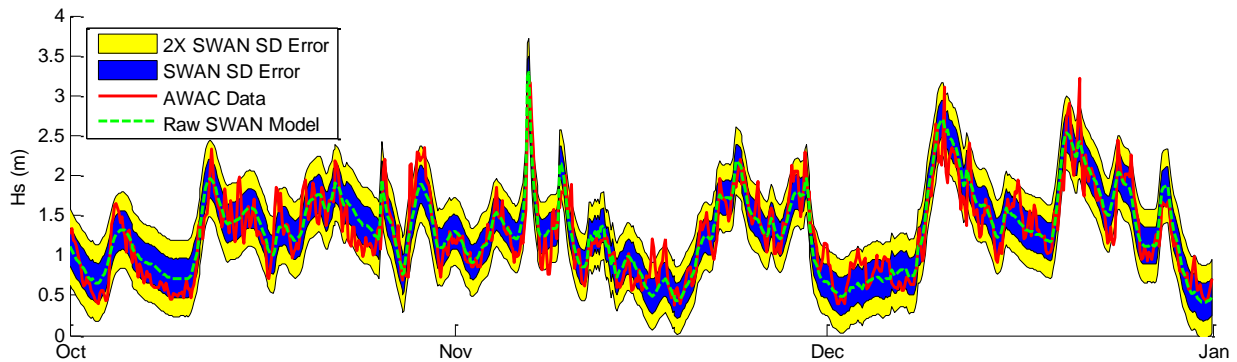


Figure 14: Comparison of ideal SWAN model confidence intervals against the AWAC dataset

5.2 Monthly calibration

Applying the monthly triple collocation parameters presented in Table 2, the SWAN model data was calibrated and the improvements, in terms of additional correlation, quantified. As shown in Figure 15 and Table 14, the resulting improvements were minimal. Table 14 illustrates the marginal improvements in correlation ($\sim 0.12\%$) when comparing the calibrated SWAN and AWAC datasets. RMSE improvements were undetectable.

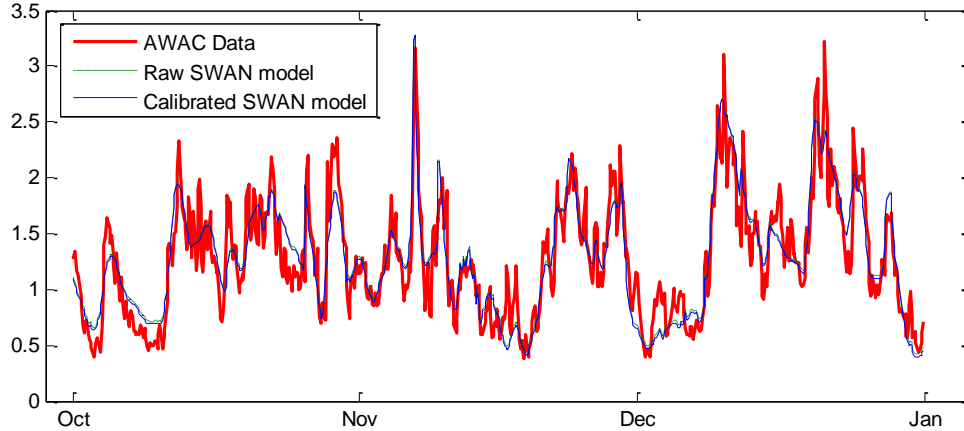


Figure 15: H_s for model calibration regime

Table 14: Correlation for Triple Collocation Method

| Correlation | Original Datasets | Calibrated Data Set | Improvement |
|--------------|-------------------|---------------------|-------------|
| SWAN vs AWAC | 0.897 | 0.899 | 0.12% |
| SWAN vs Buoy | 0.897 | 0.897 | 0.13% |
| AWAC vs Buoy | 0.999 | 0.999 | 0.00% |

5.3 Bivariate calibration

The bivariate calibration testing regime was applied to two different SWAN datasets; one at the baseline 3 hour temporal resolution and another at 1 hour temporal resolution.

Baseline SWAN model with 3 hour resolution:

Unfortunately, the baseline SWAN model suffered from a lack of data points due to the short device deployment period and the 3hr temporal resolution. As a result, triple collocation convergence results were only achieved in three out of seventeen H_s - T_e bins. This represents only a small portion of the available data. Regardless, the SWAN, AWAC and buoy datasets were calibrated, based on the bias and beta values, and the correlations between the three data sets before and after the calibration are shown in Table 15.

Table 15: Correlation between datasets under the bivariate calibration regime

| Correlation | Original Datasets | Calibrated Data Set | Improvement |
|--------------|-------------------|---------------------|-------------|
| SWAN vs AWAC | 0.858 | 0.891 | 3.99 |
| SWAN vs Buoy | 0.857 | 0.891 | 3.95 |
| AWAC vs Buoy | 0.997 | 0.997 | 0.01 |

The bivariate calibration technique results in a noticeable improvement in the correlation statistics. However, a 3.99% increase may not be sufficiently valuable to justify the increased computational requirements of the triple collocation method.

SWAN model with 1 hour resolution:

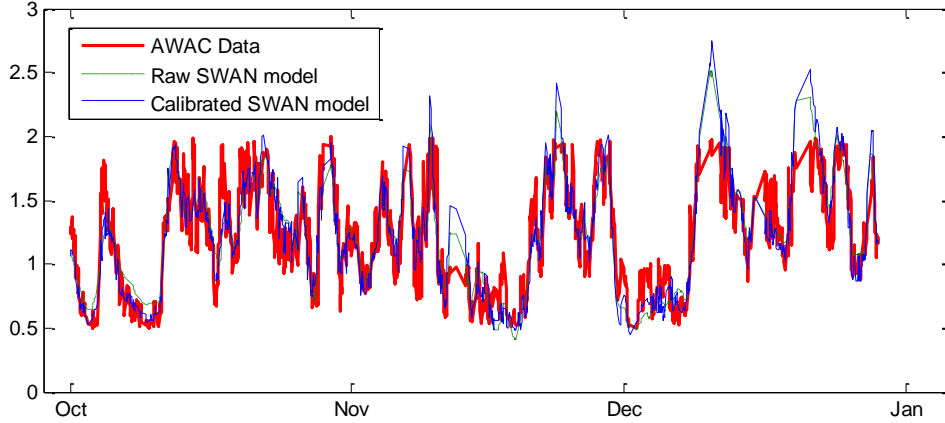


Figure 16: H_s for bivariate test regime

To improve the convergence results from the baseline SWAN model, the dataset was increased three-fold by rerunning the SWAN time at 1 hour resolution. The result dataset allowed for the triple collocation technique to achieve convergence in 62% of entire dataset. Additionally, as shown in Table 16, the use of the hourly SWAN data allows for ~5.1% increase in correlation between the calibrated SWAN and AWAC datasets. Figure 16 visually illustrates the improvements in the H_s timeseries.

Table 16: Correlation for datasets under the bivariate calibration regime

| Correlation | Original Datasets | Calibrated Data Set | Improvement |
|--------------|-------------------|---------------------|-------------|
| SWAN vs AWAC | 0.856 | 0.900 | 5.14% |
| SWAN vs Buoy | 0.856 | 0.894 | 4.44% |
| AWAC vs Buoy | 0.961 | 0.964 | 0.31% |

5.4 Spectral calibration

In the final test regime, the frequency dependent spectral variance density spectrum is calibrated, rather than the significant wave height. However, as the calibration results in Table 17 show, this calibration regime resulted in a slight reduction in performance when compared with the bivariate calibration regime. This is compounded by the much greater computational cost of the calibration regime.

Table 17: Correlation between datasets under the spectral calibration regime (2206 pairs with 1 hour resolution)

| Correlation | Original Datasets | Calibrated Data Set | Improvement |
|--------------|-------------------|---------------------|-------------|
| SWAN vs AWAC | 0.891 | 0.921 | 3.37 % |
| SWAN vs Buoy | 0.890 | 0.921 | 3.48 % |
| AWAC vs Buoy | 0.997 | 0.993 | -0.40 % |

Figure 17 below shows the significant overcorrection that occurred during the first two week of November. As a result of the spectral calibration technique, the calibrated SWAN model now predicts significant wave height of 6.8m, while the AWAC only recorded waves of 3.3 m.

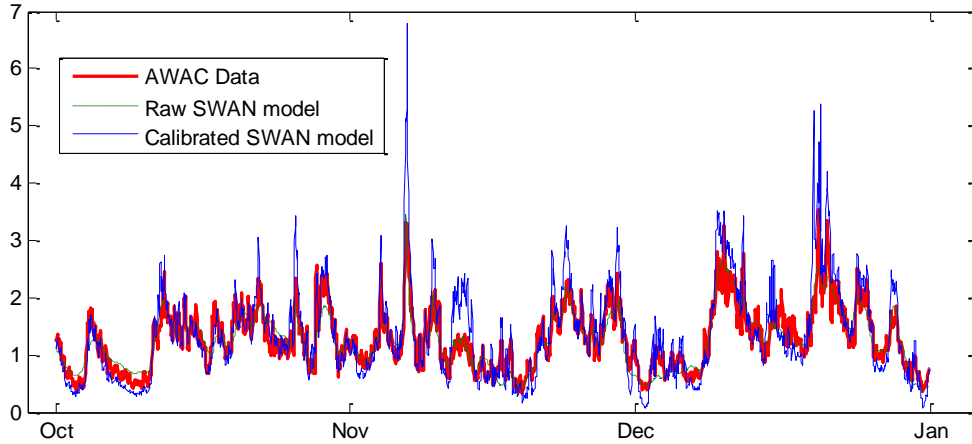


Figure 17: H_s for the spectral calibration regime

To further investigate the possible reasoning for the reduced performance of the spectral calibration regime, the correlation in each energy-frequency bin is calculated and shown in Figure 18. The majority of bins have correlation values less than 0.3, a significant reduction from the 0.89 correlation for H_s in uncalibrated dataset. If the correlation and errors strongly depend on energy and frequency level, it is expected that higher correlations would be evident in specific bins. Thus, it is postulated that other unexplored factors may have more significant influence on error variance, other than the frequency and energy level, which makes the binning non-directional spectrum to energy and frequency bins rather limited in value.

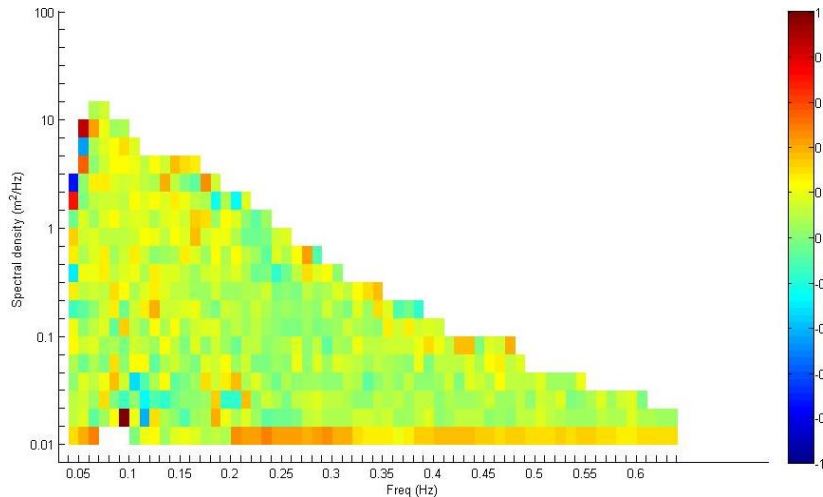


Figure 18: Correlation between AWAC and SWAN in each energy-frequency bin

5.5 Test regime performance conclusions

Based on the results presented in the previous sections, it was determined that utilizing the bivariate distribution calibration technique yield, utilizing the hourly SWAN model data, is recommended as technique which provides the best combination of calibration improvements and computational efficiency. This technique will be utilized for the remainder of the report.

Figure 19 presents the AWAC, uncalibrated and calibrated T_e SWAN values during November and December 2014. The significantly improved representative of the SWAN model T_e values is immediately evident.

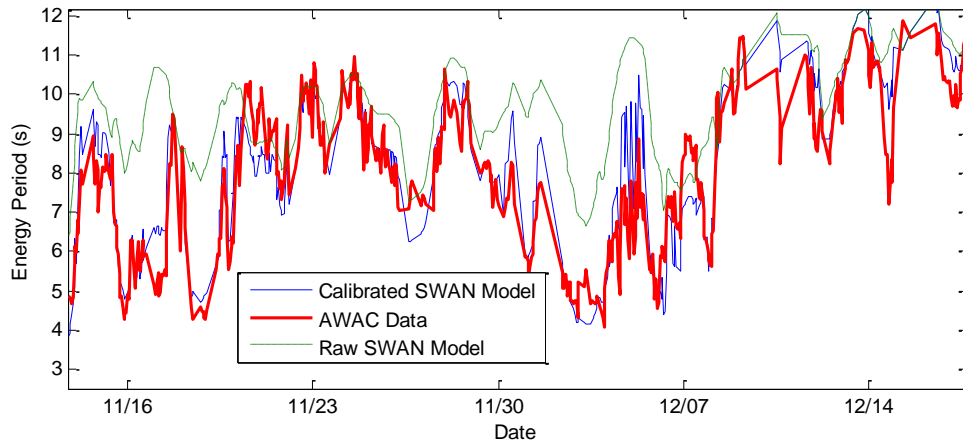


Figure 19: T_e calibration using bivariate calibration regime

6.2 Application to WEC Power Matrix

To investigate the improvement in energy production estimation for a generic WEC, the calibrated and uncalibrated SWAN model results, obtained from test regime three, are multiplied by the power matrix shown in Table 20 to calculate energy production. Readers interested in the development of the power matrix are referred to [13], [18]. Note that following results only apply to the calibrated data values – all non-calibrated data points are removed from the analysis or given a value of zero.

Table 20: WEC power matrix

| Power (kW) | Te (s) | | | | | | | | | | | | | | | | | | | |
|------------|--------|-----|-----|-----|-----|-----|------|------|------|------|------|------|------|------|------|------|------|------|------|----|
| | 4.5 | 5.5 | 6.5 | 7.5 | 8.5 | 9.5 | 10.5 | 11.5 | 12.5 | 13.5 | 14.5 | 15.5 | 16.5 | 17.5 | 18.5 | 19.5 | 20.5 | 21.5 | 22.5 | |
| Hs (m) | 0.25 | 1 | 1 | 1 | 2 | 2 | 1 | 1 | 1 | 1 | 1 | 1 | 1 | 1 | 1 | 1 | 1 | 1 | 1 | 1 |
| | 0.75 | 4 | 7 | 7 | 12 | 8 | 8 | 6 | 3 | 3 | 3 | 3 | 2 | 2 | 2 | 2 | 1 | 1 | 1 | 1 |
| | 1.25 | 9 | 11 | 19 | 32 | 22 | 23 | 14 | 24 | 7 | 5 | 9 | 5 | 11 | 4 | 6 | 3 | 3 | 2 | 3 |
| | 1.75 | 21 | 31 | 45 | 40 | 34 | 29 | 47 | 22 | 25 | 23 | 18 | 11 | 16 | 7 | 7 | 5 | 6 | 4 | 3 |
| | 2.25 | | | 93 | 99 | 110 | 104 | 39 | 63 | 30 | 41 | 20 | 22 | 25 | 15 | 26 | 15 | 11 | 3 | 7 |
| | 2.75 | | | 99 | 111 | 132 | 95 | 105 | 28 | 39 | 36 | 46 | 25 | 21 | 32 | 22 | 9 | 18 | 18 | 8 |
| | 3.25 | | | 95 | 111 | 195 | 107 | 79 | 129 | 87 | 47 | 63 | 67 | 41 | 50 | 46 | 33 | 28 | 16 | 20 |
| | 3.75 | | | 207 | 175 | 138 | 128 | 192 | 124 | 108 | 144 | 79 | 86 | 56 | 36 | 25 | 18 | 25 | 28 | 22 |
| | 4.25 | | | | 225 | 189 | 310 | 106 | 200 | 86 | 200 | 81 | 80 | 48 | 86 | 64 | 43 | 46 | 31 | 23 |
| | 4.75 | | | | | 223 | 218 | 177 | 130 | 172 | 127 | 195 | 81 | 120 | 84 | 54 | 39 | 71 | 27 | 34 |
| | 5.25 | | | | | | 344 | 323 | 253 | 282 | 192 | 195 | 109 | 137 | 73 | 45 | 69 | 45 | 61 | 38 |
| | 5.75 | | | | | | | 379 | 251 | 234 | 162 | 107 | 146 | 79 | 109 | 71 | 84 | 72 | 53 | 46 |
| | 6.25 | | | | | | | 317 | 267 | 151 | 236 | 321 | 217 | 121 | 80 | 68 | 132 | 45 | 69 | 47 |
| | 6.75 | | | | | | | 372 | 337 | 433 | 215 | 155 | 159 | 117 | 167 | 139 | 116 | 105 | 112 | 54 |
| | 7.25 | | | | | | | 479 | 375 | 237 | 224 | 307 | 168 | 180 | 110 | 147 | 127 | 74 | 58 | 79 |
| 7.75 | | | | | | | 394 | 426 | 447 | 127 | 255 | 255 | 252 | 116 | 84 | 103 | 68 | 79 | 73 | |

With the AWAC measurements as the reference dataset, the power production, correlation and bias for SWAN and buoy are shown in Table 21. As previously discussed, the triple collocation calibration method significantly increased the SWAN H_s and T_e correction. Through the calibration of the SWAN model outputs, the expected energy production increased by 2.3 MWhr or by 15.9% - a significant measure in WEC industry.

Table 21: SWAN calibration and energy production results

| | SWAN | | | Buoy | | | AWAC |
|-----------------------------|-------|------------|---------------|------|------------|---------------|------|
| | Raw | Calibrated | % Improvement | Raw | Calibrated | % Improvement | Raw |
| T_e (Correlation %) | 62.8 | 85.8 | 36.7 | 99.6 | 99.6 | 0.01 | |
| H_s (Correlation %) | 86.3 | 90.8 | 5.26 | 94.9 | 96.0 | 1.22 | |
| Energy Production (MWhr) | 14.5 | 16.8 | 15.9 | 16.5 | 16.5 | 0.01 | 16.5 |
| Energy Production Bias (MW) | -2.00 | 0.30 | 85.0 | 0.00 | 0.00 | 0.00 | |

Calibrated and raw uncalibrated SWAN model power time series are shown in Figure 20. While the calibrated SWAN model correlates better with the AWAC reference dataset, it is noticeable that the calibrated SWAN model over predicts power production as several time during the 3 month period. The discussion in Section 7 will provide additional discussion around these over predicted values.

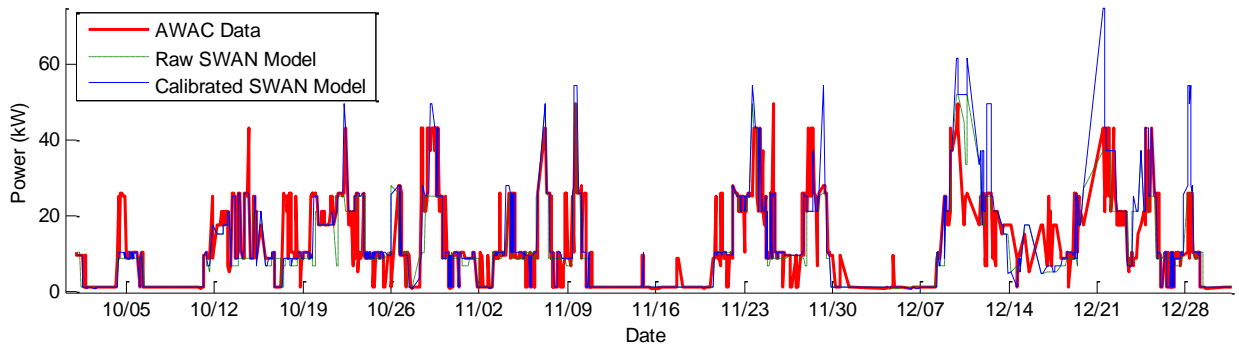


Figure 20: Calibrated SWAN model power production

The detailed statistical comparison between the calibrated and original power time series is shown in Table 22. The calibrated power correlation is improved by 10%, while bias drops from -1.44 kW to 0.26kW.

Table 22: Calibrated data power time series comparison

| | Calibrated Power | Original Power |
|-------------------|------------------|----------------|
| Mean Value (kW) | 12.0 | 12.0 |
| Bias to AWAC (kW) | 0.26 | -1.44 |
| RMSE | 7.19 | 7.64 |
| Scatter Index | 0.60 | 0.64 |
| Correlation | 0.80 | 0.72 |
| Pairs | 1376.0 | 1376.0 |

6.3 Impact of Annual WEC Energy Production

In order to estimate the impact of calibrating the SWAN model on annual energy production estimates, rather than just the 3 month data collection period, the annual wave resource histogram for 2014 was calibrated using the 11 convergence histogram bins in Table 13 - which accounts for 62% of wave conditions during 2014. Using the calibration parameters obtained from bivariate calibration regime, the calibrated histogram is shown in Table 23. As a result of the calibration, the resulting histogram is more diffuse and values are spread across a larger number H_s and T_e bins.

Table 23: Calibrated SWAN Histogram

| | | Calibrated SWAN Histogram | | | | | | | | | | | | | | | |
|--------------------|-------|---------------------------|---|---|---|-----|----|-----|-----|-----|-----|----|----|----|----|----|----|
| | | Te (s) | | | | | | | | | | | | | | | |
| | | 1 | 2 | 3 | 4 | 5 | 6 | 7 | 8 | 9 | 10 | 11 | 12 | 13 | 14 | 15 | 16 |
| H _s (m) | 0-0.5 | | | | | 8 | | 35 | 31 | 16 | | | | | | | |
| | 0.5-1 | | | | | 341 | 19 | 411 | 176 | 80 | 29 | | | | | | |
| | 1-1.5 | | | | | | | 56 | 77 | 113 | 159 | | | | | | |
| | 1.5-2 | | | | | | | 3 | 19 | 33 | 32 | 78 | 55 | | | | |
| | 2-2.5 | | | | | | | | 13 | 10 | 12 | 3 | | | | | |
| | 2.5-3 | | | | | | | | | | | | | | | | |
| | 3-3.5 | | | | | | | | | | | | | | | | |
| | 3.5-4 | | | | | | | | | | | | | | | | |

Figure 21 plots the time-series of power production from both calibrated and original data. It is noted that the calibration generally increases the under predicted larger waves during winter, and decreases the over predicted smaller waves during the summer months. The resulting annual energy production (purely on the calibrated seastates) decreases from 32.6 MWhr to 30.5 MWhr, a gross reduction of 6.4 %. It is noted that negative bias values in Table 10 never result in a negative significant height value, thereby justifying the inclusion of bias in (1).

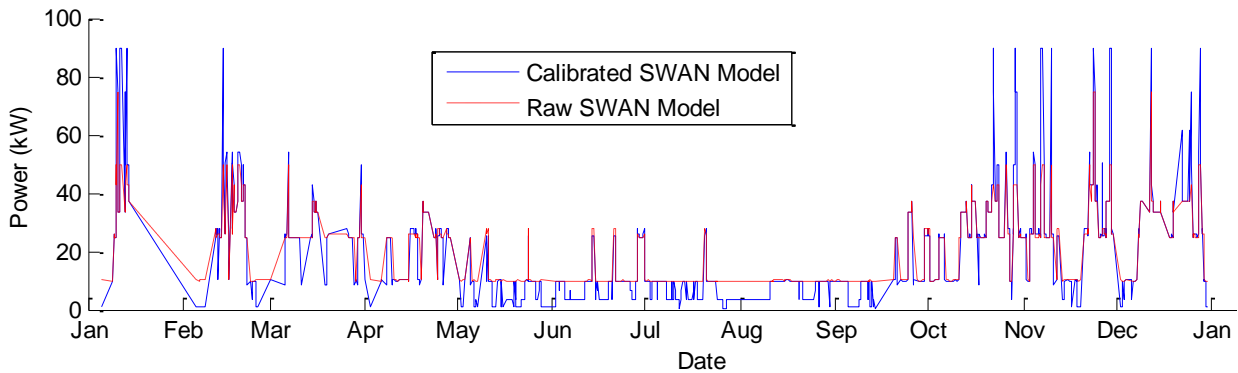


Figure 21: Calibrated and original SWAN data for entire year

7 Discussion

As shown in Figure 20 and Figure 22, the calibrated significant wave heights occasionally perform worse than their uncalibrated counterparts. For example, in Figure 22, raw SWAN model over predicts the 3.5m peak on November 6th, 2014 by ~0.25 meter, yet the calibrated SWAN over predicts the peak by 1m. Similar behaviour is noted on December 21st.

During both of these storm events, the number of bivariate histogram bin occurrences is relatively low and results in contradictory results. The 3.25m H_s bin containing both these storm events contains only contains five observation hours. As shown in Table 24, SWAN over predicts H_s in two out of five hours data and under predicts H_s in the other three hours. Therefore, the triple collocation technique will calibrate the data in the 3.25m bin by increasing the significant wave height values.

Table 24: Conflicting correlation bias's for single bivariate bin

| Date & Time | Nov 6, 22:00 | Nov 6, 23:00 | Nov 7, 00:00 | Dec 21, 04:00 | Dec 21, 05:00 | Average |
|-------------|--------------|--------------|--------------|---------------|---------------|---------|
| AWAC | 3.17 | 3.02 | 3.28 | 3.10 | 3.11 | 3.14 |
| SWAN | 3.42 | 3.23 | 2.73 | 2.31 | 2.37 | 2.812 |
| Bias | 0.251 | 0.212 | -0.553 | -0.793 | -0.736 | -0.324 |

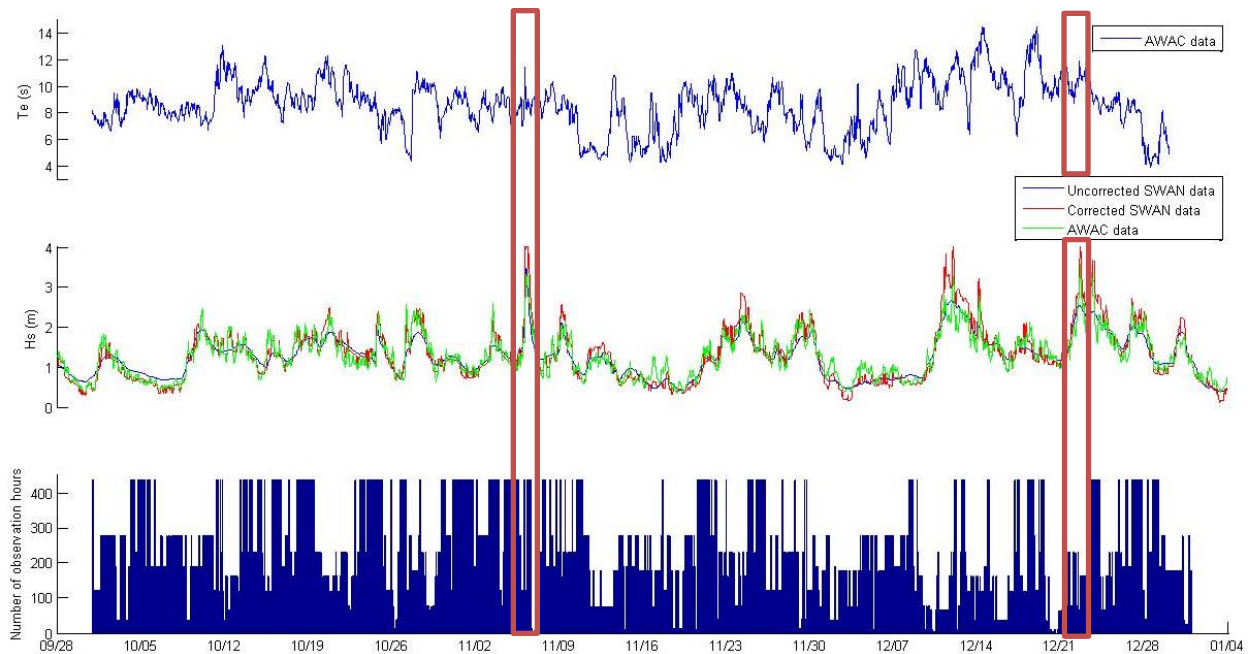


Figure 22: AWAC, uncalibrated SWAN, calibrate SWAN, and number of observation hours

This result can be attributed to two factors; Firstly, the assumption behind the bivariate calibration regime is that measurement error of wave measurement devices and numerical models only depend on the significant wave height and energy period of the wave. However, in reality, this measurement error can be affected by multiple factors such as currents, local wind, multi-modal seastate, and other influencing factors. Secondly, larger sample size in individual bin is needed to reduce the effect from random outliers and obtain a normal distribution for error.

8 Conclusion

Numerical wave propagation models are often used to hindcast wave conditions and predict the theoretical energy production from wave energy conversion (WEC) devices. It is widely acknowledged that numerical model suffer from bias's and uncertainties which ultimately significantly affect the final predictions of WEC power. In this case study, a Simulating Waves Nearshore (SWAN) model is used to predict sea states at Canada west coast off Vancouver Island and the triple collocation technique is applied to quantify the model result bias's, and systematic and random errors.

This study implemented two previously utilized calibration regimes and two novel calibration regimes. The single value and monthly calibration regime were first presented by Caires and Sterl[5] and Janssen et al. [6] respectively. While the calibrated SWAN models resulting from the first two methods did not result in improved model performance, they highlighted the need for larger datasets and the confirmed that the error was normally distributed – a key assumption of the triple collocation technique.

The bivariate calibration regime resulted in the greatest improvement in significant wave height correlation (5.14%), with the more computationally intensive spectral calibration regime only achieving 2.5% improvement. The results mean 0.30 correlation between the calibrated SWAN model and AWAC,

across the entire frequency domain variance density spectrum, from the spectral calibration regime is well below the 0.89 from the raw uncalibrated H_s values thus indicating the frequency and variance density do not capture all factors which influence the model uncertainties.

In accordance with the calibration regime results, it was determined that the bivariate calibration method outperformed the other investigated regimes was utilized for the remainder of the study. Applied to T_e , SWAN / AWAC correlation improved by 29%. Applying the resulting improved wave resource assessment data to WEC power matrix increased the 3 month energy production by 15.9% and reduced the under prediction SWAN bias to just 0.30% (when compared against the AWAC data). If the calibration seastates were applied on an annual basis, the annual energy production differs 6 percent between calibrated SWAN data and original data – a significant amount when assessing large scale wave energy production.

9 Acknowledgements

This work has been funded by Natural Resources Canada and Natural Sciences and Engineering Research Council of Canada. This funding is gratefully acknowledged. Additionally, the authors would like to thank Jean Bidlot at ECMWF for providing the necessary boundary condition data to run the SWAN model

10 References

- [1] E. B. L. Mackay, A. S. Bahaj, and P. G. Challenor, “Uncertainty in wave energy resource assessment. Part 1: Historic data,” *Renew. Energy*, vol. 35, no. 8, pp. 1792–1808, 2010.
- [2] M. Portabella and a. Stoffelen, “On Scatterometer Ocean Stress,” *J. Atmos. Ocean. Technol.*, vol. 26, no. 2, pp. 368–382, 2009.
- [3] T. H. Durrant, D. J. M. Greenslade, and I. Simmonds, “Validation of Jason-1 and Envisat remotely sensed wave heights,” *J. Atmos. Ocean. Technol.*, vol. 26, no. 1, pp. 123–134, 2009.
- [4] G. Muraleedharan, a D. Rao, M. Sinha, and D. K. Mahapatra, “Analysis of Triple Collocation Method for validation of model predicted significant wave height data,” vol. 10, no. 2, pp. 79–84, 2006.
- [5] S. Caires, “Validation of ocean wind and wave data using triple collocation,” *J. Geophys. Res.*, vol. 108, no. C3, pp. 1–16, 2003.
- [6] P. a E. M. Janssen, S. Abdalla, H. Hersbach, and J. R. Bidlot, “Error estimation of buoy, satellite, and model wave height data,” *J. Atmos. Ocean. Technol.*, vol. 24, no. 9, pp. 1665–1677, 2007.
- [7] K. Scipal, T. Holmes, R. De Jeu, V. Naeimi, and W. Wagner, “A possible solution for the problem of estimating the error structure of global soil moisture data sets,” *Geophys. Res. Lett.*, vol. 35, no. 24, pp. 2–5, 2008.

- [8] B. Robertson, C. Hiles, and B. Buckham, "Characterizing the Nearshore Wave Energy Resource on the West Coast of Vancouver Island," *Renew. Energy*, vol. 71, pp. 665–678, 2013.
- [9] L. H. Holthuijsen, N. Booji, J. G. Haagsma, a. T. M. M. Kieftenburg, R. C. Ris, a. J. van derWesthuysen, and M. Zijlema, "USER MANUAL SWAN Cycle III version 40.51," *Cycle*, p. 137, 2006.
- [10] B. Robertson, H. Bailey, D. Clancy, J. Ortiz, and B. Buckham, "Influence of wave resource assessment methodology on wave energy production estimates," *Renew. Energy*, vol. 86, pp. 1145–1160, 2016.
- [11] R. F. Marsden, "A Proposal for a Neutral Regression," *J. Atmos. Ocean. Technol.*, vol. 16, no. 7, pp. 876–883, 1999.
- [12] W. D. Wilson and E. Siegel, "Current and wave measurements in support of the Chesapeake Bay Interpretive Buoy System," *2011 IEEE/OES/CWTM 10th Work. Conf. Curr. Waves Turbul. Meas. CWTM 2011*, no. May, pp. 94–99, 2011.
- [13] B. Robertson, H. Bailey, D. Clancy, J. Ortiz, and B. Buckham, "Influence of Wave Resource Assessment Methodology on Wave Energy Production Estimates," vol. 1, no. 250, pp. 1–27.
- [14] I. E. C. T. C. 114 IEC, "Wave energy resource assessment and characterization.," *IEC/TS 62600-101*. 2014.
- [15] A. Cornett and J. Zhang, "Nearshore Wave Energy Resources, Western Vancouver Island, B.C.," Canadian Hydraulics Centre, 2008.
- [16] B. Robertson, C. Hiles, and B. Buckham, "Characterizing the Nearshore Wave Energy Resource on the West Coast of Vancouver Island.," *Renew. Energy*, vol. In submiss, 2013.
- [17] P. Lenee-Bluhm, R. Paasch, and H. T. Özkan-Haller, "Characterizing the wave energy resource of the US Pacific Northwest," *Renew. Energy*, vol. 36, no. 8, pp. 2106–2119, 2011.
- [18] H. Bailey, J. Ortiz, B. Robertson, B. Buckham, and R. Nicoll, "A methodology for wave-to-wire WEC simulations," *Marine Renewable Energy Technology Symposium*. Seattle, WA, 2014.